

# Automated Fat Quantification Applied to Abdominal MR Images

Q. Peng<sup>1</sup>, R. W. McColl<sup>2</sup>, P. T. Weatherall<sup>2</sup>

<sup>1</sup>Radiology, UT Health Science Center at San Antonio, San Antonio, TX, United States, <sup>2</sup>Radiology, UT Southwestern Medical Center, Dallas, TX, United States

## INTRODUCTION

Fat distribution measurement on human is of great significance for a cluster of obesity-related diseases (such as diabetes, cardiovascular disease) generally referred to as metabolic syndrome. Also, monitoring the change of fat distribution longitudinally for patients with metabolic syndrome, after pharmaceutical intervention or life style change, is of great importance for improved drug development and disease treatment. Rapid and accurate fat quantification on MR images obtained in the human abdomen has been a challenge due to the poor contrast between fat and non-fat in traditional non-water-suppressed images. Therefore, rapid automated or semi-automated fat quantification methods have difficulties achieving reliable fat volume measurement. Manual contour drawing still seems to be the most accepted approach for fat quantification, although it is slow, and suffers greatly from inter- and intra-observer variations. In addition, partial volume effects can not be accurately evaluated using a manual contour drawing method. Recently, a rapid MR fat imaging technique based on water-saturated balanced steady-state free precession (b-SSFP) has been proposed to generate high quality, fat-only images (1). It has been shown this technique can achieve high contrast between fat and non-fat, which has the propensity to make accurate and automated fat quantification possible.

## METHODS AND RESULTS

### 1. Automated Fat Quantification Method

Due to the limited spatial resolution of MRI, lipid tissue can be distributed in a full volume, and can co-exist with water and/or air tissue in the context of abdominal fat imaging. In an ideal water-suppressed image (neglecting residual water signal, noise, and other imaging imperfections such as  $B_0$  and  $B_1$  inhomogeneities), signal intensity from a voxel full of fat would generate maximum signal ( $S_{max}$ , with  $N_1$  pixels) in the image, and the signal intensity from a voxel partially filled with fat would be proportional to the volume ratio of fat in that pixel. Full volume voxels are mainly the static bulk fat, such as subcutaneous fat. Partial-volume fat pixels are located mainly at fat tissue interfaces, and the lower signal can be due to partial volume fat filling, or to intestinal motion. Due to the complicated fat distribution and potential intestinal motion, the distribution of the partial-volume fat signal on a histogram is not predictable. However, if the number of pixels in an image is large enough (or imaging resolution is high), the probability that a given pixel has a signal intensity less than  $S_{max}$  is close to equal. Thus, a uniform (or rectangular) distribution with pixel density  $N_2$  can be used to approximate the partial-volume fat signal distribution, as shown in Fig. 1. Assuming a Gaussian noise distribution,  $N_1$ ,  $N_2$  can be obtained easily via curve fitting on the image histogram. Because on average, partial-volume voxels are half filled, a theoretical fat volume can be calculated as follows: Total Fat Volume (TFV) =  $(N_1 + N_2 * S_{max}/2) \times$  Full Voxel Size. Therefore, a corresponding signal threshold which best separates fat and non-fat can be determined as:  $S_{th} = S_{max}/2$ . Fat volume can be determined as: TFV =  $(N_1 + S_{th} \times N_2) \times$  Full Voxel Size.

### 2. Validation Method

The same human abdominal phantom and 3D WS b-SSFP pulse sequence in (1) were used here. Briefly, the phantom had dual-layered concentric cylinders with known internal/external/total oil volumes of 3.16L/6.34L/9.50L. Six datasets were obtained. A signal threshold ( $Th_{fp}=S_{th}=S_{max}/2$ ) was automatically determined for each image via curve fitting to separate fat voxels from background and other tissues. To compare this fat quantification method with a traditional method which includes mainly full-volume fat pixels, another threshold was determined to be  $Th_{full}=S_{max}-\sigma$ . Based on the binary fat-only images obtained by the two thresholds, internal-, external-, and total- oil volumes were calculated via ROI analyses. A single factor analysis of variance (Anova) was used to determine whether the two techniques predicted significantly different oil volumes. A  $P$  value of less than 0.05 was considered statistically significant.

Tab. 1. Phantom Meas. Results (Vol. in % of true volume)

Repeat	Internal		External		Total	
	$Th_{full}$	$Th_{fp}$	$Th_{full}$	$Th_{fp}$	$Th_{full}$	$Th_{fp}$
1	89.6	100.0	95.4	102.5	93.4	101.6
2	88.7	100.0	94.9	102.4	92.8	101.6
3	89.7	99.2	95.0	102.6	93.3	101.5
4	89.0	100.0	95.3	102.6	93.2	101.7
5	89.7	100.2	95.3	102.4	93.4	101.7
6	88.4	101.0	95.4	103.0	93.1	102.3
Mean	89.2	100.1	95.2	102.6	93.2	101.7
SD	0.5	0.6	0.2	0.2	0.2	0.3
$P$	<0.0001		<0.0001		<0.0001	

## Discussion

How fat distribution correlates with these diseases is still a very controversial subject. This is partially related to the limitations of currently available techniques, including both human fat distribution imaging method and fat quantification (post-processing) methods. The fat quantification method proposed here is verified to be fast and accurate on phantom. *In vivo* results are also consistent with the phantom results (not shown). This technique, in combination with the rapid 3D WS b-SSFP fat imaging method (1), can lead to much easier and more accurate fat quantification on human.

## REFERENCES

1. Peng Q, McColl R, et al, JMRI, 2005; 21(3):263-71

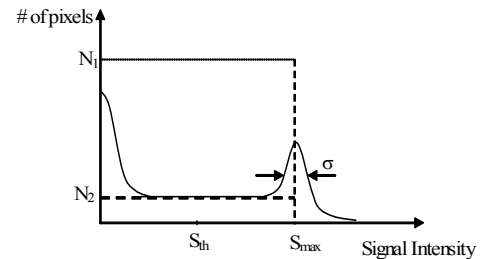


Fig. 1. Theoretical and expected histogram of a fat image. Dashed lines show the theoretical histogram as predicted by the full- and partial-volume fat distribution model. Solid line shows the expected histogram of a water-saturated MR image, due to imaging noise, background artifacts, and residual water signal.  $N_1$ : number of full fat voxels;  $N_2$ : density of partial fat voxels;  $\sigma$ : FWHM of fat peak.

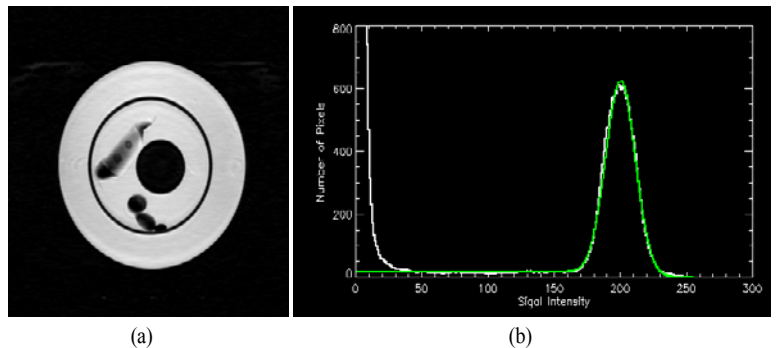


Fig. 2. Representative phantom image and its histogram. The image in (a) was obtained using 3D WS b-SSFP sequence on the human abdomen phantom. In the histogram plot (b), the white curve represents the histogram of the image, and the green curve represents the result of curve fitting.

## 3.

### Results

A representative phantom image obtained using the 3D WS b-SSFP sequence is demonstrated in Fig. 2a. The corresponding histogram and the curve fitting result are illustrated in Fig. 2b. As shown earlier (1), water signal is effectively suppressed using WS b-SSFP, and the corresponding signal is close to the noise level centered at zero. Full-voxel fat signal distribution agrees well with a Gaussian-shape peak. Partial-voxel fat signal is between fat peak signal and zero, and a uniform distribution is obtained, consistent with the previous uniform distribution assumption for partial-volume fat voxels. The phantom oil volume measurement results using two different threshold methods are shown in Tab. 1. It is shown that the two processing methods resulted in significantly different accuracies on phantom oil volume estimation. The  $Th_{full}$  method leads to a mean underestimation of 10.8% for IAF, and 4.8% for SAF. The  $Th_{fp}$  method proposed herein which considered both full- and partial-volume fat generated much closer estimation of true oil volumes. The mean deviations of IAF and SAF oil volumes are only 0.1% and 2.6%, respectively.